Submitted to the Annals of Applied Statistics

PROBABILITY AGGREGATION: DYNAMIC HIERARCHICAL MODELING OF EXPERT BELIEFS IN GEOPOLITICAL EVENTS

BY VILLE A. SATOPÄÄ, SHANE T. JENSEN, LYLE H. UNGAR, BARBARA A. MELLERS, AND PHIL E. TETLOCK

Department of Statistics, The Wharton School of the University of Pennsylvania
E-mail: satopaa@wharton.upenn.edu; stjensen@wharton.upenn.edu
Department of Computer and Information Science, University of Pennsylvania
E-mail: ungar@cis.upenn.edu
Department of Psychology, University of Pennsylvania
E-mail: mellers@wharton.upenn.edu; tetlock@wharton.upenn.edu

Most subjective probability aggregation procedures use a single probability judgement from each expert, even though it is common for experts studying real problems to update their probability estimates over time. This paper makes an advance towards unexplored areas of probability aggregation by considering a dynamic context in which experts are allowed to update their beliefs at random intervals. The updates are assumed to occur very infrequently, resulting into a highly sparse dataset that cannot be modeled by standard time-series procedures. In response to the lack of appropriate methodology, this paper presents a dynamic model that takes into account the forecasters level of self-reported expertise and produces aggregate probabilities that are sharp and well-calibrated both in- and out-of-sample. The model is demonstrated on a real-world dataset that includes over 2,300 experts making multiple probability forecasts on different subsets of 166 different international political events.

1. Introduction. Individual experts can differ radically from one another in their abilities to assess probabilities of future events. The quality of a probability assessment is typically evaluated in regards to an important attribute called *calibration*. An expert is said to be well-calibrated if his probabilities match with the long-term frequencies of the events. This means that, for instance, the proportion of events that actually occurred is 60% for all those events for which he assessed a probability of 0.60. Even though several experiments have been conducted to show that experts are generally poorly calibrated (see, e.g., Cooke (1991); Shlyakhter et al. (1994)), expertise has been found to be associated with calibration. In particular, Wright et al. (1994) argue that a higher level of self-reported expertise on the subject matter implies better calibration.

Unfortunately, calibration by itself does not guarantee usefulness. To see this, consider a relatively stationary process, such as rain in some geographic region, whose empirical frequency of occurrence in the last 10 years is 45%. In this setting an expert can assess a constant probability of

Keywords and phrases: Probability Aggregation, Dynamic Linear Model, Hierarchical Modeling, Expert Forecast, Subjective Probability, Bias Estimation, Calibration, Time Series

0.45 and be well-calibrated. This probability, however, is close to 0.5 and hence too uninformative to be very useful in decision making. For the sake of comparison, consider another expert whose typical probability assessment is near 0.0 or 1.0. In the forecasting literature such an expert is called *sharp*. If the expert is not only sharp but also well-calibrated, then he is able to forecast the behavior of the process both with high certainty and accuracy. From the decision-maker's perspective, his advice is highly useful as it involves very little risk and much information. For these reasons, a common goal in probability estimation is to maximize sharpness subject to calibration (see, e.g., Raftery et al. (2005); Ranjan and Gneiting (2010)). This is a well-defined goal that has led to a wide range of novel and insightful observations in probability forecasting literature.

One such observation is related to the aggregation of multiple probabilities. There is strong empirical evidence that bringing together the strengths of different experts by combining their probability forecasts into a single consensus, known as the *crowd belief*, results in better predictive performance. Being motivated by the long list of applications of probability forecasts, including medical diagnosis (Wilson et al. (1998); Pepe (2003), political and socio-economic foresight (Tetlock (2005)), and meteorology (Sanders (1963); Vislocky and Fritsch (1995); Baars and Mass (2005)), researchers have proposed many different approaches to combining probability forecasts (see, e.g., Ranjan and Gneiting (2010); Satopää et al. (2013) for some recent studies, and Genest and Zidek (1986); Wallsten, Budescu and Erev (1997); Clemen and Winkler (2007); Primo et al. (2009) for a comprehensive overview). The general focus, however, has been on developing one-time aggregation procedures that consult the expert's advice only once before the event resolves.

Consequently, many areas of probability aggregation still remain rather unexplored. For instance, consider an investor aiming to assess whether a stock index will finish trading above some threshold on a given date. In order to maximize his overall predictive accuracy, he may consult a group of experts repeatedly over a period of time and adjust his estimate of the aggregate probability accordingly. Since the experts are allowed to update their probability assessments, the aggregation should be performed by taking into account the temporal correlation in their advice. Many standard time-series procedures could be used to perform this aggregation as long as the experts update their advice consistently on a daily basis.

This paper adds another layer of complexity by assuming a heterogeneous set of experts, most of whom only make one or two probability assessments over the hundred or so days before the event resolves. The problem at hand is therefore strikingly different from many time-series estimation problems, where one has an observation at every time point – or almost every time point. Therefore standard time-series procedures like ARIMA (see, e.g., Mills (1991)) are not applicable without ignoring the heterogeneity among the experts. In response to the lack of procedures to model sparse and heterogeneous probability forecasting data, this paper introduces an interpretable time-series model that incorporates self-reported expertise and captures a sharp and well-calibrated estimate of the crowd belief. The model is then used for

- the analysis of group-level under- and overconfidence across different levels of self-reported expertise,
- accurate probability forecasts, and

Statistic	Min.	Q_1	Median	Mean	Q_3	Max.
# of Days a Problem is Active	4	35.6	72.0	106.3	145.20	418
# of Experts per Problem	212	543.2	693.5	783.7	983.2	1690
# Forecasts given by each Expert on a Problem	1	1.0	1.0	1.8	2.0	131
# Problems participated by an Expert	1	14.0	36.0	55.0	90.0	166

TABLE 1

Five-number summaries of our real-world data.

Expertise Level	1	2	3	4	5
Frequency (%)	25.3	30.7	33.6	8.2	2.1

TABLE 2

Frequencies of the self-reported expertise (1 = Not At All Expert and 5 = Extremely Expert) levels across all the 166 questions in our real-world data.

- many question-specific quantities that have easy interpretations and can be used to gain novel insight in the social sciences.

The paper begins with a description of our probability forecasting data that were collected by asking over 2,300 experts to give probability forecasts and to self-assess their level of expertise on a subset of 166 geopolitical binary events. After summarizing the dataset, the paper introduces a dynamic hierarchical model for capturing the crowd belief. The model is estimated in a two-step procedure. First, constrained parameter estimates are obtained via Gibbs sampling (see Geman and Geman (1984) for the original introduction of Gibbs sampling). These estimates are then transformed to their unconstrained equivalents by a calibration step. An extension of this model to polychotomous outcomes is briefly discussed before model evaluation. The first evaluation section uses synthetic data to study the accuracy to which the two-step procedure is able to estimate parameter values. The second evaluation section discusses different aspects of the model by applying it to our real-world probability forecasting data. The paper concludes with a discussion on future research directions and model limitations.

2. Geopolitical Forecasting Data. The data collection began with a recruitment of 2,365 forecasters ranging from graduate students to political science faculty and practitioners. The recruiting was made from professional societies, research centers, alumni associations, science bloggers, and word of mouth. Requirements included at least a Bachelor's degree and completion of psychological and political tests that took roughly two hours. These measures assessed cognitive styles, cognitive abilities, personality traits, political attitudes, and real-world knowledge. The experts were asked to give probability forecasts (to the second decimal point) and to self-assess their level of expertise (measured on a 1-to-5 scale with 1 = Not At All Expert and 5 = Extremely Expert) on a number of 166 geopolitical binary events taking place between September 29, 2011 and May 8, 2013. Each question was active for a period of time during which the participating experts were allowed to update their forecasts as frequently as they liked without being penalized. The forecast-

ers knew that their probability estimates would be assessed for accuracy using Brier scores[1]. This incentivized them to report their true beliefs instead of attempting to game the system (Winkler and Murphy (1968)). In addition to receiving $150 for meeting minimum participation requirements that did not depend on prediction accuracy, the forecasters also received status rewards for their performance via leader-boards displaying Brier scores for the top 20 forecasters. Since a typical expert participated only in a small subset of the 166 questions, the forecasters are considered indistinguishable conditional on the self-reported level of expertise. Tables 1 and 2 provide more relevant summary statistics on the data. Notice that the distribution of the self-reported expertise is skewed to the right and that some questions remained active longer than others. For more details on the data and its collection see Ungar et al. (2012).

(a) *Will the expansion of the European bailout fund be ratified by all 17 Eurozone nations before 1 November 2011?*

(b) *Will the Nikkei 225 index finish trading at or above 9,500 on 30 September 2011?*

FIG 1. *Scatterplots of the probability forecasts given for two questions in our dataset. The shadings represents the self-reported expertise of the forecaster who provided the probability forecast.*

To illustrate the nature of the data with some concrete examples, Figures 1(a) and 1(b) show scatterplots of the probability forecasts given for (a) *Will the expansion of the European bailout fund be ratified by all 17 Eurozone nations before 1 November 2011?*, and (b) *Will the Nikkei 225 index finish trading at or above 9,500 on 30 September 2011?*. The points have been jittered slightly to make overlaps visible. The darkness of the points are positively associated with the self-

[1]The Brier score is the squared distance between the probability forecast and the event indicator that equals 1.0 or 0.0 depending on whether the event happened or not, respectively. See Brier (1950) for the original introduction.

reported expertise levels. Given that the European bailout fund was ratified before 1 November 2011 and that the Nikkei 225 index finished trading at around 8,700 on 30 September 2011, the general trend of the probability forecasts converge to the correct answers. There is, however, much disagreement among the experts. This disagreement persists even near the closing dates of the questions. Unfortunately, the data is not only noisy but also quite sparse. As mentioned before, the forecasters were allowed to update their forecast as long as the questions remained active. Updating was done on a very infrequent basis. An expert gave, on average, only 0.0159 forecasts per day, and so a typical expert made a forecast about every 62 days. As a result the average response rate was around 13.5 forecasts per day from a large group of experts.

3. Model. Let $p_{i,t,k} \in (0,1)$ be the probability forecast given by the ith expert at time t for the kth question, where $i = i, \ldots, I_k$, $t = 1, \ldots, T_k$, and $k = 1, \ldots, K$. Denote the logit-probabilities with

$$Y_{i,t,k} = \text{logit}(p_{i,t,k}) = \log\left(\frac{p_{i,t,k}}{1-p_{i,t,k}}\right) \in \mathbb{R}$$

and collect the logit-probability forecasts given for question k at time t into a vector $\boldsymbol{Y}_{t,k} = [Y_{1,t,k}\ Y_{2,t,k}\ \ldots\ Y_{I_k,t,k}]^T$. Partition the experts into J groups based on some individual feature, such as self-reported expertise, with each group sharing a common multiplicative bias term $b_j \in \mathbb{R}$ for $j = 1, \ldots, J$. Collect these bias terms into a bias vector $\boldsymbol{b} = [b_1\ b_2\ \ldots\ b_J]^T$ and let $\boldsymbol{M}_k$ be a $I_k \times J$ matrix denoting the group-memberships of the forecasters in question k. That is, if the ith expert participating in the kth question belongs to the jth group, then the ith row of $\boldsymbol{M}_k$ is the jth standard basis vector, $\boldsymbol{e}_j$. The bias vector $\boldsymbol{b}$ does not include a subindex because it is considered shared among all the K questions. To secure model identifiability, it is sufficient to share only one of the elements of $\boldsymbol{b}$ among the questions. This element defines a baseline under which it is possible to estimate the remaining $J-1$ bias terms separately within each of the questions. In this paper, however, the entire vector $\boldsymbol{b}$ is shared because some of the questions in our real-world data set involve very few experts with the highest level of self-reported expertise. Under this notation, the model for the kth question can be expressed as

$$\boldsymbol{Y}_{t,k} = \boldsymbol{M}_k \boldsymbol{b} X_{t,k} + \boldsymbol{v}_{t,k} \tag{1}$$

$$X_{t,k} = \gamma_k X_{t-1,k} + w_{t,k} \tag{2}$$

$$X_{0,k} \sim \mathcal{N}(\mu_0, \sigma_0^2)$$

where Equation (1) denotes the observed process, Equation (2) shows the hidden process that is driven by the constant $\gamma_k \in \mathbb{R}$. The error terms are independent and identically distributed normal random variables with mean zero

$$\boldsymbol{v}_{t,k}|\sigma_k^2 \overset{i.i.d.}{\sim} \mathcal{N}_{I_k}(\boldsymbol{0}, \sigma_k^2 \boldsymbol{I}_{I_k})$$

$$w_{t,k}|\tau_k^2 \overset{i.i.d.}{\sim} \mathcal{N}(0, \tau_k^2),$$

and $(\mu_0, \sigma_0^2) \in (\mathbb{R}, \mathbb{R}^+)$ are hyper-parameters chosen *a priori*. The hidden state $X_{t,k}$ represents the sharp and calibrated logit-probability for the kth event given the information available up to and including time t. To make this more specific, let $Z_k \in \{0, 1\}$ indicate whether the event associated with the kth question happened ($Z_k = 1$) or did not happen ($Z_k = 0$). If $\{\mathcal{F}_{t,k}\}_{t=1}^{T_k}$ is a filtration representing the information available up to and including a given time point, then $\mathbb{E}[Z_k|\mathcal{F}_{t,k}] = \mathbb{P}(Z_k = 1|\mathcal{F}_{t,k}) = \text{logit}^{-1}(X_{t,k})$. These probabilities are made estimable by assuming that the observed process is associated with the filtration $\{\mathcal{F}_{t,k}\}_{t=1}^{T_k}$ and hence can be used as a proxy for the amount of information available at any given time point. Therefore it is not unreasonable to interpreted the hidden process as the crowd belief across time.

To give intuitive interpretations of the other model parameters, notice that the error term in the observed process has mean zero. Therefore the forecasters are assumed to be, on average, a multiplicative constant $\boldsymbol{b}$ away from the calibrated crowd belief. An individual element of $\boldsymbol{b}$ can be interpreted as a group-specific *systematic bias* that labels the group either as over-confident ($b_j \in (1, \infty)$) or as under-confident ($b_j \in (0, 1)$). Unfortunately, due to the high sparsity of our data, estimating a bias term and analyzing the bias separately for each expert is not possible. See Section 7.3 for an analysis and discussion on the bias terms. Any other deviation from the calibrated crowd belief is considered *random noise*. This noise is measured in terms of σ_k^2 and can be assumed to be caused by momentary over-optimism (or pessimism), false beliefs, or other misconceptions.

Similarly to the observed process, the hidden process has a systematic and a random component. The *random fluctuations* are measured in terms of τ_k^2 and can be assumed to represent changes or shocks to the underlying circumstances that ultimately decide the outcome of the event. The *systematic component* γ_k, on the other hand, allows the model to incorporate a constant signal stream that drifts the hidden process to infinity (when $\gamma_k \in (1, \infty)$) or zero (when $\gamma_k \in (0, 1)$). If the uncertainty in the question diminishes as the current time point t approaches T_k, the hidden process drifts to infinity. Alternatively, the hidden process can drift to zero in which case any available information about the target event does not improve predictive accuracy. Since each of the K questions in our dataset was resolved within a pre-specified timeframe, γ_k is expected to fall within the interval $(1, \infty)$ for all $k = 1, \ldots, K$.

4. Model Estimation. The most challenging part of our model estimation is to incorporate the event indicators $\{Z_k\}_{k=1}^K$ such that the hidden process is well-calibrated and the interpretability of our model is not compromised. This section introduces a two-step procedure, called *Sample-Then-Calibrate* or simply *STC*, that achieves this goal in a flexible and efficient manner by first estimating the model parameters under a constraint (*Sampling Step*) and then performing a one-dimension optimization procedure to transform the constrained estimates into their unconstrained counterparts (*Calibration Step*).

4.1. *Sampling Step.* Since $\left(a\boldsymbol{b}, X_{t,k}/a, a^2\tau_k^2\right) \neq \left(\boldsymbol{b}, X_{t,k}, \tau_k^2\right)$ for any $a > 0$ yield the same likelihood for $\boldsymbol{Y}_{t,k}$, the model as described by Equations (1) and (2) is not identifiable and the parameter estimates tend to drift during the sampling process. A well-known solution is to choose one of the elements of $\boldsymbol{b}$, say b_3, as the reference point and fix $b_3 = 1$. Denote the constrained

version of the model by

$$\begin{aligned}
\boldsymbol{Y}_{t,k} &= \boldsymbol{M}_k \boldsymbol{b}(1) X_{t,k}(1) + \boldsymbol{v}_{t,k} \\
X_{t,k}(1) &= \gamma_k(1) X_{t-1,k}(1) + w_{t,k} \\
\boldsymbol{v}_{t,k} | \sigma_k^2(1) &\overset{i.i.d.}{\sim} \mathcal{N}_{I_k}(\boldsymbol{0}, \sigma_k^2(1) \boldsymbol{I}_{I_k}) \\
w_{t,k} | \tau_k^2(1) &\overset{i.i.d.}{\sim} \mathcal{N}\left(0, \tau_k^2(1)\right),
\end{aligned}$$

where the trailing input parameter emphasizes the constraint $b_3 = 1$. Since this version is identifiable, estimates of the model parameters can be obtained. Denote the estimates by placing a hat on the parameter symbol. For instance, $\hat{\boldsymbol{b}}(1)$ and $\hat{X}_{t,k}(1)$ represent the estimates of $\boldsymbol{b}(1)$ and $X_{t,k}(1)$, respectively. These estimates are found via a Gibbs sampler that only makes use of standard distributions. See Appendix A for the technical details of our sampler, and, e.g., Gelman et al. (2003) for a discussion on the general principles of Gibbs sampling.

4.2. *Calibration Step.* Since the model parameters can be estimated under a constrained version of b_3, the next step is to determine how b_3 should be constrained such that both the sharpness and calibration of the estimated hidden process are maximized. This section introduces an efficient procedure that finds the optimal constraint without requiring any additional runs of the sampling step. First, assume that parameter estimates $\hat{\boldsymbol{b}}(1)$ and $\hat{X}_{t,k}(1)$ have already been obtained via the constrained sampling step described in Section 4.1. Since for any $\beta \in \mathbb{R}/\{0\}$,

$$\begin{aligned}
\boldsymbol{Y}_{t,k} &= \boldsymbol{M}_k \boldsymbol{b}(1) X_{t,k}(1) + \boldsymbol{v}_{t,k} \\
&= \boldsymbol{M}_k \left(\boldsymbol{b}(1)\beta\right) \left(X_{t,k}(1)/\beta\right) + \boldsymbol{v}_{t,k} \\
&= \boldsymbol{M}_k \boldsymbol{b}(\beta) X_{t,k}(\beta) + \boldsymbol{v}_{t,k},
\end{aligned}$$

the parameter values under $b_3 = \beta$ can be obtained from $\boldsymbol{b}(\beta) = \boldsymbol{b}(1)\beta$ and $X_{t,k}(\beta) = X_{t,k}(1)/\beta$. This means that $X_{t,k} = X_{t,k}(1)/\beta$ when β is equal to the true value of b_3. Since the hidden process $X_{t,k}$ is assumed to be sharp and well-calibrated, b_3 can be estimated by the value of β that simultaneously maximizes the sharpness and calibration of $\hat{X}_{t,k}(1)/\beta$. A natural criterion for this maximization is provided by the class of *proper scoring rules* that combine sharpness and calibration (Gneiting et al. (2008); Buja, Stuetzle and Shen (2005)). Due to the possibility of *complete separation* in any one question (see, e.g., Gelman et al. (2008)), the maximization must be performed over multiple questions. Therefore we estimate

$$\hat{\beta} = \underset{\beta \in \mathbb{R}/\{0\}}{\arg\max} \sum_{k=1}^{K} \sum_{t=1}^{T_k} S\left(Z_k, \hat{X}_{k,t}(1)/\beta\right) \tag{3}$$

where $Z_k \in \{0, 1\}$ indicate whether the event associated with the kth question happened ($Z_k = 1$) or did not happen ($Z_k = 0$). The function S is a strictly proper scoring rule such as the negative Brier score (Brier (1950))

$$S_{BRI}(Z, X) = -(Z - \text{logit}^{-1}(X))^2$$

or the logarithmic score (Good (1952))

$$S_{LOG}(Z, X) \quad = \quad Z \log\left(\text{logit}^{-1}(X)\right) + (1 - Z) \log\left(1 - \text{logit}^{-1}(X)\right)$$

Since it is not clear which rule should be used for predicting geopolitical events, such as the ones in our dataset, the *Sample-Then-Calibrate* procedure is evaluated separately under both rules in Sections 6 and 7. Once $\hat{\beta}$ has been computed, estimates of the unconstrained model parameters are given by

$$\begin{aligned}
\hat{X}_{t,k} &= \hat{X}_{k,t}(1)/\hat{\beta} \\
\hat{\boldsymbol{b}}_{t,k} &= \hat{\boldsymbol{b}}(1)\hat{\beta} \\
\hat{\tau}_k^2 &= \hat{\tau}_k^2(1)\hat{\beta}^2 \\
\hat{\sigma}_k^2 &= \hat{\sigma}_k^2(1) \\
\hat{\gamma}_k &= \hat{\gamma}_k(1)
\end{aligned}$$

Notice that the parameters σ_k^2 and γ_k are not affected by the constraint. Therefore their constrained and unconstrained estimates are the same.

4.3. *Discussion.* If the class labels in the data are balanced with respect to the time points, the calibration step with the logarithmic scoring rule is approximately equivalent to *Platt calibration*, which has been shown to yield good calibration under various modeling scenarios (see, e.g., Platt et al. (1999); Niculescu-Mizil and Caruana (2005)). To see this, recall that the Platt calibrated logit-probabilities are given by $\hat{A} + \hat{B}\hat{X}_{t,k}(1)$, where

$$\left(\hat{A}, \hat{B}\right) = \underset{A,B\in\mathbb{R}}{\arg\max} \sum_{k=1}^{K} \sum_{t=1}^{T_k} S_{LOG}(Z_k, A + B\hat{X}_{t,k}(1)) \tag{4}$$

This is equivalent to fitting a logistic regression model with Z_k as the response and $\hat{X}_{t,k}(1)$ as the explanatory variable. To understand the behavior of the coefficients A and B, express the logistic regression as linear regression

$$\text{logit}(\mathbb{P}(Z_k = 1|\hat{X}_{t,k})) = A + B\hat{X}_{t,k} + e_{t,k}$$

with $e_{t,k} \overset{i.i.d.}{\sim} \mathcal{N}(0, \sigma^2)$. If the data are balanced with respect to the time points, then exactly half of the summands in Equation (4) have $Z_k = 1$ and the average response logit-probability $\text{logit}(\mathbb{P}(Z_k = 1|\hat{X}_{t,k}))$ is close to zero. Since the values of $\hat{X}_{t,k}$ are estimated logit-probabilities of the same K events across different time points, their overall average is also around zero. Therefore both the response and explanatory variables are approximately centered. This means that the intercept term A is near zero reducing Platt calibration to Equation (3) under the logarithmic scoring rule. If the data is not balanced, Platt calibration can be easily incorporated into our model via an additional intercept parameter. This, however, reduces the interpretability of our model. Fortunately, compromising interpretability is rarely necessary because it is often possible to use the data in a well-balanced form. One procedure to attain this is described in the beginning of Section 7.

5. Extension: Polychotomous Outcomes. If the future event can take upon $M > 2$ possible outcomes, the hidden state $X_{t,k}$ must be extended to a vector of size $M-1$. One of the outcomes, e.g., the Mth one, is chosen as the base-case. This gives us a total of $M-1$ observed processes and one hidden process

$$\begin{aligned}
\boldsymbol{Y}_{1,t,k} &= \boldsymbol{M}_k \boldsymbol{b}_1 X_{1,t,k} + \boldsymbol{v}_{1,t,k} \\
\boldsymbol{Y}_{2,t,k} &= \boldsymbol{M}_k \boldsymbol{b}_2 X_{2,t,k} + \boldsymbol{v}_{2,t,k} \\
&\vdots \\
\boldsymbol{Y}_{M-1,t,k} &= \boldsymbol{M}_k \boldsymbol{b}_{M-1} X_{M-1,t,k} + \boldsymbol{v}_{M-1,t,k} \\
\boldsymbol{X}_{t,k} &= \gamma_k^T \boldsymbol{I}_{M-1} \boldsymbol{X}_{t-1,k} + \boldsymbol{w}_{t,k}
\end{aligned}$$

where $\boldsymbol{X}_{t,k}$ is a $(M-1) \times 1$ matrix of calibrated logit-probabilities. Notice that each process has a separate bias vector. The error terms are independent and identically distributed multivariate normal random variables

$$\begin{aligned}
\boldsymbol{v}_{m,t,k} | \sigma^2_{j,k} &\overset{i.i.d.}{\sim} \mathcal{N}_{I_k}\left(\boldsymbol{0}, \sigma^2_{j,k} \boldsymbol{I}_{I_k}\right) \\
\boldsymbol{w}_{t,k} | \tau^2_k &\overset{i.i.d.}{\sim} \mathcal{N}_{M-1}\left(\boldsymbol{0}, \tau^2_k \boldsymbol{I}_{M-1}\right)
\end{aligned}$$

On the left-hand side of observed process

$$\begin{aligned}
\boldsymbol{Y}_{m,t,k} &= \begin{bmatrix} Y_{m,1,t,k} & Y_{m,2,t,k} & \dots & Y_{m,I_k,t,k} \end{bmatrix}^T \\
&= \begin{bmatrix} \log\left(\frac{p_{m,1,t,k}}{p_{M,1,t,k}}\right) & \log\left(\frac{p_{m,2,t,k}}{p_{M,2,t,k}}\right) & \dots & \log\left(\frac{p_{m,I_k,t}}{p_{M,I_k,t,k}}\right) \end{bmatrix}^T
\end{aligned}$$

is a $I_k \times 1$ matrix of the expert logit-probabilities for the mth outcome of the kth question at time t, and on the left-hand side of the hidden process

$$\boldsymbol{X}_{t,k} = \begin{bmatrix} X_{1,t,k} & X_{2,t,k} & \dots & X_{M-1,t,k} \end{bmatrix}^T$$

is the matrix of sharp and calibrated logit-probabilities at time t. Choosing one of the outcomes as the base-case, ensures that the probabilities will sum to one at any given time point. Since this multinomial extension is equivalent to having $M-1$ independent binary-outcome models (see Section 3), the estimation can be done separately for each outcome. Therefore, even though this paper focuses on modeling binary events, all the properties and discussion generalize to the multi-outcome case.

6. Synthetic Data Results TODO . The synthetic data is not generated directly from the model for several reasons: (i) showing good performance on a dataset directly generated from the model assumptions is hardly any news, and (ii) generating data from the dynamic model description does not produce calibrated hidden states. The latter is important for our interpretation of the hidden

states as the calibrated crowd belief. In order to achieve this, let $\{Z_{t,k}\}_{t=1}^{T_k}$ denote the values of a standard Brownian motion at time points $t = 1, \ldots, T_k, T_k$. Then,

$$\begin{aligned} Z_k &= \mathbb{1}\left(Z_{T_k,k} > 0\right) \\ X_{t,k} &= \text{logit}\left[\Phi\left(\frac{Z_{t,k}}{\sqrt{T_k - t}}\right)\right] \end{aligned}$$

Once the hidden process has been generated, the expert logit forecasts are produced by adding white noise to the given sequences of $X_{t,k}$.

The simulation is performed over a four-dimensional grid of values: The number of questions, K, varies between $10, 25, 50, 75$, and 100, the values of β change from 0.5 to 1.5 with steps of size 0.25, the values of α range from -0.5 to 0.5 with steps of size 0.25, and finally the values of σ^2 vary from 0.25 to 1.5 with steps of size 0.25. At each grid point the simulation runs a total of two times; each time measuring how well the approaches estimate the hidden process in terms of quadratic loss. The average loss from the two runs is used as the performance measure at that grid point. Since the final results are summarized by choosing one of the grid variables (e.g. α) and then averaging over the remaining three variables (e.g. β, K, and σ^2), each average value in the final results represents an average of a $2 \times 5^3 = 250$ values.

Figure 2 summarizes the results by choosing one grid variable at a time and then averaging over the remaining three variables. The *Sample-Then-Calibrate* with log loss outperforms the other two approaches almost uniformly across the grid.

7. Geopolitical Data Results. This section discusses results related to the real-world data described in Section 2. The goal is to provide application specific insight by discussing the specific research objectives itemized in Section 1 and also to evaluate the *Sample-Then-Calibrate*-procedure in terms of predictive power and calibration. Before presenting the results two practical matters are discussed.

The first matter regards human experts making probability forecasts of 0.0 or 1.0 even when they are not completely sure of the outcome of the future event. For instance, all the 166 questions in our dataset contained both a zero and a one. Transforming such forecasts into the logit-space yields infinities that are highly influential and cause problems in model estimation. To avoid this, Ariely et al. (2000) suggest changing $p = 0.0$ and 1.0 to $p = 0.02$ and 0.98, respectively. This is similar to winsorising which sets the extreme probabilities to a specified percentile of the data (see, e.g., Hastings et al. (1947) for more details on winsorising). Allard, Comunian and Renard (2012), on the other hand, consider only probabilities that fall within a constrained interval, say $[0.001, 0.999]$, and discard the rest. Since this implies ignoring a portion of the data, we decided to adopt the first approach by changing $p = 0.0$ and 1.0 to $p = 0.01$ and 0.99, respectively.

The second matter is related to the distribution of the class labels in the dataset. If the set of events that occurred is much larger than the set of events that did not occur (or *vice versa*), the dataset is called *imbalanced*. On such data the model can end up over-focusing on the larger class, and as a result, give very accurate forecast performance over the larger class at the cost of performing poorly over the smaller class (see, e.g., Chen (2009); Wallace and Dahabreh (2012)).

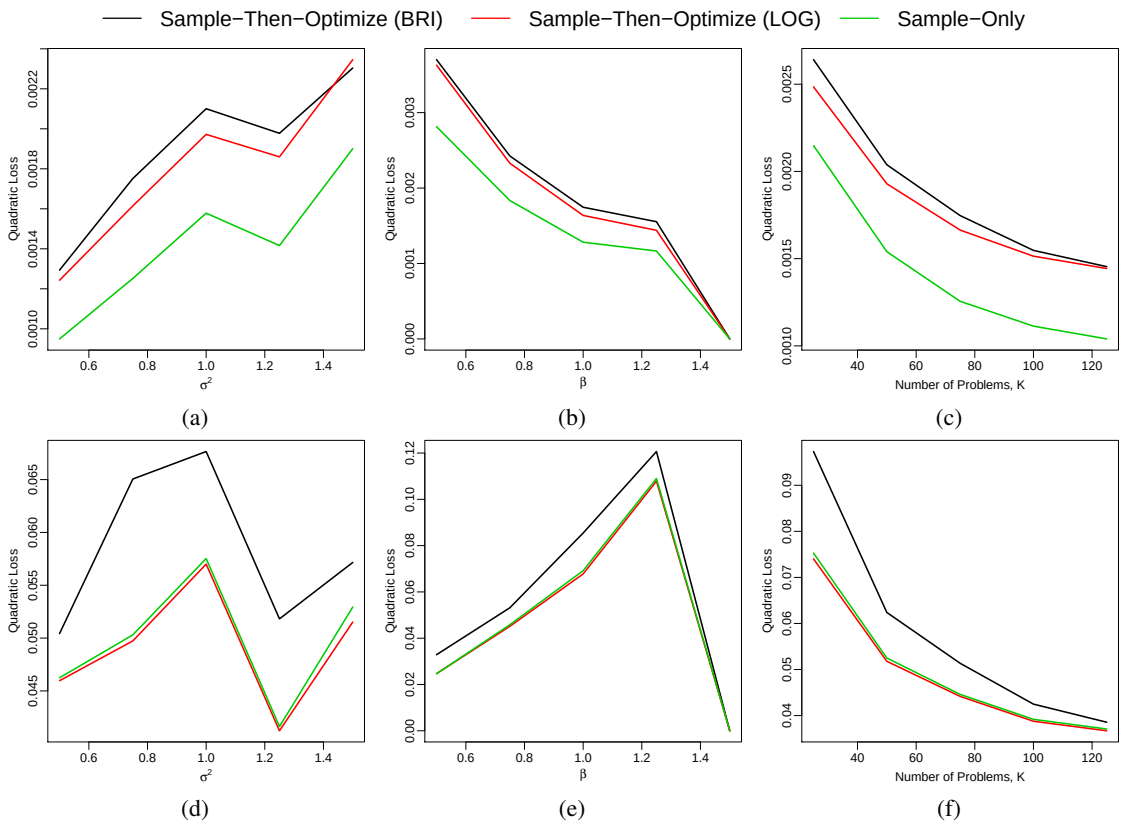

FIG 2. *Comparing the approaches on synthetic data. (a) Performance under different values of* σ^2*. (b) Performance under different values of* α*. (c) Performance under different values of* β*. (d) Performance under different numbers of questions,* K*.*

Fortunately, it is often possible to detect a well-balanced form of the dataset. The first step is to find a partition, S_0 and S_1, of the question indices, $\{1, 2, \ldots, K\}$, such that the equality $\sum_{k \in S_0} T_k = \sum_{k \in S_1} T_k$ is as closely approximated as possible. This is equivalent to an NP-hard problem known in computer science as the *Partition Problem*: determine whether a given set of positive integers can be partitioned into two sets such that the sums of the two sets equal to each other (see, e.g., Karmarkar and Karp (1982); Hayes (2002)). A simple solution is to use a greedy algorithm, which iterates through the values of T_k in descending order, assigning each T_k to the subset that currently has the smaller sum (see, e.g. Kellerer, Pferschy and Pisinger (2004); Gent and Walsh (1996) for more details on the Partition Problem). After finding a well-balanced partition, the next step is to assign the class labels such that the labels for the questions in S_x are equal to x with $x = 0$ or 1. Recall from section 4.2 that Z_k represents the event indicator for the event associated with the kth

question. To define a balanced set of indicators, for all $k \in S_x$, let

$$\tilde{Z}_k = x$$
$$\tilde{p}_{i,t,k} = \begin{cases} 1 - p_{i,t,k} & \text{if } Z_k = 1 - x \\ p_{i,t,k} & \text{if } Z_k = x \end{cases}$$

with $i = 1, \ldots, I_k$, and $t = 1, \ldots, T_k$. The set $\left\{ \left(\tilde{Z}_k, \{\tilde{p}_{i,t,k} | i = 1, \ldots, I_k, t = 1, \ldots, T_k\} \right) \right\}_{k=1}^{K}$ is a balanced version of the data. This procedure was used to balance our real-world dataset both in terms of events and time points. The final output splits the events exactly in half ($|S_0| = |S_1| = 83$) such that number of time points in the first and second halves are 8,737 and 8,738, respectively.

7.1. *Out-of-Sample Forecasting.* This section evaluates the out-of-sample predictive performance of *Sample-Then-Calibrate* against several other probability aggregation procedures. All the models are allowed to utilize a training set before making predictions on an independent testing set. In order to clarify some of the upcoming notation, let S_{train} and S_{test} be index sets that partition the data into training and testing sets of sizes $|S_{train}| = N_{train}$ and $|S_{test}| = 166 - N_{test}$, respectively. This means that the kth question is in the training set if and only if $k \in S_{train}$. The competing models are as follows.

1. *Simple Dynamic Linear Model (SDLM).* This procedure fixes $\boldsymbol{b} = \mathbf{1}$ and $\beta = 1$ in the hierarchical model described in Section 3. The model then reduces to

$$\begin{aligned} \boldsymbol{Y}_{t,k} &= X_{t,k} + \boldsymbol{v}_{t,k} \\ X_{t,k} &= \gamma_k X_{t-1,k} + w_{t,k}, \end{aligned}$$

   where $X_{t,k}$ is the logit-probability used for prediction. Since this model is not hierarchical, estimates of the hidden process can be obtained directly for the questions in the testing set without fitting the model first on the training set. In order to make predictions, the sampler is run for 500 iterations of which the first 200 are used for burn-in. The remaining sample of 300 iterations is thinned by discarding every other observation, leaving a final predictive sample of 150 observations.
2. *The Sample-Then-Calibrate procedure both under the Brier (STC-Bri) and the logarithmic score (STC-Log).* The model is first fit on the training set by running the sampling step for 3,000 iterations of which the first 500 iterations are used for burn-in. After thinning by only keeping every fifth observation, the calibration step is performed for each of the remaining 500 observations. The out-of-sample prediction is done by running the sampling step for 500 iterations with each consecutive iteration reading in and conditioning on the next value of β and $\boldsymbol{b}$ that were found during training period. The first 200 observations are used for burn-in. The remaining sample of 300 iterations is thinned by discarding every other observation, leaving a final predictive sample of 150 observations.

3. *A fully Bayesian version of STC-Log (BSTC-Log).* Denote the (constrained) calibrated logit-probabilities and the event indicators across all K questions with $\boldsymbol{X}(1)$ and $\boldsymbol{Z}$, respectively. The posterior distribution of β conditional on $\boldsymbol{X}(1)$ is then given by $p(\beta|\boldsymbol{X}(1), \boldsymbol{Z}) \propto p(\boldsymbol{Z}|\beta, \boldsymbol{X}(1))p(\beta|\boldsymbol{X}(1))$. Recall that the calibration step under S_{LOG} is equivalent to fitting a logistic regression model with Z_k as the response and $\hat{X}_{k,t}(1)$ as the explanatory variable. Therefore the likelihood for the Bayesian version is

$$p(\boldsymbol{Z}|\beta, \boldsymbol{X}(1)) \propto \prod_{k=1}^{K}\prod_{t=1}^{T_k} \text{logit}^{-1}\left(X_{k,t}(1)/\beta\right)^{Z_k}\left(1-\text{logit}^{-1}\left(X_{k,t}(1)/\beta\right)\right)^{1-Z_k} \tag{5}$$

   Similarly to Gelman et al. (2003) the prior is chosen to be locally uniform, $p(1/\beta) \propto 1$. Posterior estimates of β can be sampled from Equation (5) using generic sampling algorithms such as the Metropolis algorithm (Metropolis et al. (1953)) or slice sampling (Neal (2003)). Since the sampling procedure conditions on the event indicators, the full conditional distribution of the hidden states is a non-standard form. Therefore the Metropolis algorithm is also used for sampling the hidden states. Predictions are made with the same choices of thinning and burn-in as described under *Sample-Then-Calibrate*.
4. Due to the lack of previous literature on dynamic aggregation of expert probability forecasts, the main competitors are exponentially weighted versions of procedures that have been proposed for static probability aggregation:
   (a) *Exponentially Weighted Moving Average (EWMA).* If

$$\bar{p}_{t,k} = \frac{1}{N_{t,k}}\sum_{i=1}^{N_{t,k}} p_{i,t,k},$$

   is the average probability forecast given at time t for the kth question, then the EWMA forecasts for the kth problem are obtained recursively from

$$\hat{p}_{t,k}(\alpha) = \begin{cases} \bar{p}_{1,k} & \text{for } t = 1 \\ \alpha\bar{p}_{t,k} + (1-\alpha)\hat{p}_{t-1,k}(\alpha) & \text{for } t > 1 \end{cases}$$

   where the input parameter α is learned from the training set by

$$\hat{\alpha} = \underset{\alpha\in[0,1]}{\arg\min} \sum_{k\in S_{train}}\sum_{t=1}^{T_k}\left(Z_k - \hat{p}_{t,k}(\alpha)\right)^2$$

   (b) *Exponentially Weighted Moving Logit Aggregator (EWMLA).* This is a moving version of the aggregator $\hat{p}_G(\boldsymbol{b})$ that was introduced in Satopää et al. (2013). If $\boldsymbol{p}_{t,k}$ is a vector collecting all the probability forecasts made for the kth question at time t, then the EWMLA forecasts are found recursively from

$$\hat{p}_{t,k}(\alpha, \boldsymbol{b}) = \begin{cases} G_{t,k}(\boldsymbol{b}) & \text{for } t = 1 \\ \alpha G_{t,k}(\boldsymbol{b}) + (1-\alpha)\hat{p}_{t-1,k}(\alpha, \boldsymbol{b}) & \text{for } t > 1 \end{cases}$$

where

$$G_{t,k}(\nu) \quad = \quad \left(\prod_{i=1}^{N_{t,k}} \left(\frac{p_{i,t,k}}{1-p_{i,t,k}} \right)^{\frac{\boldsymbol{e}_{i,k}'\boldsymbol{b}}{N_{t,k}}} \right) \Bigg/ \left(1 + \prod_{i=1}^{N_{t,k}} \left(\frac{p_{i,t,k}}{1-p_{i,t,k}} \right)^{\frac{\boldsymbol{e}_{i,k}'\boldsymbol{b}}{N_{t,k}}} \right)$$

The vector $\boldsymbol{b}$ collects the bias terms of the different expertise groups. Therefore it is equivalent to the bias vector found under *Sample-Then-Calibrate*. The term $\boldsymbol{e}_{i,k}$ is a vector of length 5 indicating which level of self-reported expertise the ith forecaster in the kth question belongs to. For instance, if $\boldsymbol{e}_{i,k} = [0,1,0,0,0]$, then the expert identifies himself with the expertise level two. The tuning parameters $(\alpha, \boldsymbol{b})$ are learned from the training set by

$$(\hat{\alpha}, \hat{\boldsymbol{b}}) \quad = \quad \underset{\boldsymbol{b}\in\mathbb{R}^5, \alpha\in[0,1]}{\arg\min} \sum_{k\in S_{train}} \sum_{t=1}^{T_k} (Z_k - \hat{p}_{t,k}(\alpha, \boldsymbol{b}))^2$$

(c) *Exponentially Weighted Moving Beta-transformed Aggregator (EWMBA)*. The static version of the Beta-transformed (linear) aggregator was introduced in Ranjan and Gneiting (2010). A dynamic version can be obtained by replacing $G_{t,k}(\nu)$ in the EWMLA description with

$$H_{\nu,\tau}\left(\bar{p}_{t,k}\right),$$

where $H_{\nu,\tau}$ is the cumulative distribution function of the Beta distribution and $\bar{p}_{t,k}$ is the average probability forecast defined under EWMA. The tuning parameters (α, ν, τ) are learned from the training set by

$$(\hat{\alpha}, \hat{\nu}, \hat{\tau}) \quad = \quad \underset{\nu,\tau>0\ \alpha\in[0,1]}{\arg\min} \sum_{k\in S_{train}} \sum_{t=1}^{T_k} (Z_k - \hat{p}_{t,k}(\alpha, \nu, \tau))^2$$

The competing models are evaluated via a 10-fold cross-validation[2] that first partitions the 166 questions into 10 sets. The partition is chosen such that each of the 10 sets has approximately the same number of questions (16 or 17 questions per set in our case) and the same number of time points (between 1760 and 1764 time points per set in our case). The evaluation then iterates 10 times, each time using one of the 10 sets as the testing set and the remaining 9 sets as the training set. Each question is therefore used nine times for training and exactly once for testing. The testing proceeds sequentially one testing question at a time as follows: First, for a question with a time horizon of T_k, make a prediction based on the first two days. Compute the Brier score for the aggregate forecast of the second day. Next, make a prediction based on the first three days and

[2] A 5-fold cross-validation was also performed. The results were, however, very similar to the 10-fold cross-validation and hence not presented in the paper.

compute the Brier score for the most recent day, namely, the third day. Repeat this process until the prediction is made on all of the $T_k - 1$ days. This leads to $T_k - 1$ Brier scores per testing question and a total of 17,475 Brier scores across the entire dataset.

Table 3 summarizes different ways to aggregate these scores: The first option, denoted by *Scores by Day*, weighs the questions by the number of days the question remained open. This is performed by computing the average of the 17,475 scores. The second option, denoted by *Scores by Problem*, gives each question an equal weight regardless how long the question remained open. This is done by first averaging the scores within a question, and then averaging the average scores across all the questions. Both scores can be further broken down into subcategories by considering the length of the questions. The questions are divided into *Short* questions (30 days or fewer), *Medium* questions (between 31 and 59 days), and *Long* Problems (60 days or more). The number of questions in these subcategories were 36, 32 and 98, respectively. The bolded scores indicate the lowest score in each column. The values in the parenthesis quantify the variability in the scores: Under *Scores by Day* the values give the standard errors of all the scores. Under *Scores by Problem*, on other hand, the values represent the standard errors of the average scores across the questions.

Scores by Day

Model	All Problems	Short	Medium	Long
SDLM	0.100 (0.156)	0.066 (0.116)	0.098 (0.154)	0.102 (0.157)
BSTC-Log	0.097 (0.213)	**0.053** (0.147)	0.100 (0.215)	0.098 (0.215)
STC-Bri	0.096 (0.190)	0.056 (0.134)	0.097 (0.190)	0.098 (0.192)
STC-Log	**0.096** (0.191)	0.056 (0.134)	**0.096** (0.189)	**0.098** (0.193)
EWMBA	0.102 (0.203)	0.060 (0.124)	0.110 (0.201)	0.103 (0.206)
EWMLA	0.102 (0.199)	0.061 (0.130)	0.111 (0.214)	0.103 (0.200)
EWMA	0.111 (0.142)	0.089 (0.100)	0.111 (0.136)	0.112 (0.144)

Scores by Problem

Model	All Problems	Short	Medium	Long
SDLM	0.089 (0.116)	0.064 (0.085)	0.106 (0.141)	0.092 (0.117)
BSTC-Log	0.083 (0.160)	**0.052** (0.103)	0.110 (0.198)	0.085 (0.162)
STC-Bri	0.083 (0.142)	0.055 (0.096)	0.106 (0.174)	0.085 (0.144)
STC-Log	**0.082** (0.142)	0.055 (0.096)	**0.105** (0.174)	**0.085** (0.144)
EWMBA	0.090 (0.156)	0.063 (0.101)	0.118 (0.186)	0.091 (0.161)
EWMLA	0.090 (0.159)	0.064 (0.109)	0.120 (0.200)	0.090 (0.159)
EWMA	0.104 (0.105)	0.092 (0.081)	0.119 (0.125)	0.103 (0.107)

TABLE 3

Brier Scores based on 10-fold cross-validation. Scores by Day weighs a question by the number of days the question remained open. Scores by Problem gives each question an equal weight regardless how long the question remained open. The bolded values indicate the lowest scores in each column. The values in the parenthesis represent standard errors in the scores.

Overall, STC-Bri and STC-Log achieve the lowest average scores across all columns except *Short* where they are slightly outperformed by BSTC-Log. BSTC-Log, however, turns out to be overconfident (see Section 7.2 with a discussion on calibration and sharpness). This means that BSTC-Log underestimates the uncertainty in the events and outputs probability forecasts that are typically too near 0.0 or 1.0 to be calibrated. As a result, the forecasts are either very close to the

correct answer or very far from it. As can be seen in Table 3, this results into high variance in performance of BSTC-Log. The short questions, however, involve very little uncertainty and were generally the easiest to forecast. On such easy questions, overconfidence can pay off frequently enough to compensate for the few potential large scores that arise from an overconfident and incorrect forecast. In contrast to the BSTC-Log-model, SDLM lacks sharpness and is highly underconfident. This means that SDLM makes conservative forecasts that result into low average scores and low performance variability. The *Sample-Then-Calibrate*-model can therefore be viewed as a well-performing compromise that avoids over-confidence without being too conservative.

Of the exponentially weighted moving aggregators, EWMBA performs the best and EWMA the worst. Given that the static versions of EWMLA and EWMBA depend on similar transformations, the results suggest that EWMLA is unable to make efficient use of the self-rated expertise information. Both EWMLA and EWMBA, however, suffer from over-confidence and are therefore unable to outperform the *Sample-Then-Calibrate*-model.

The dataset contained a few long questions with an abrupt change of the crowd belief from one answer option to another. Since these abrupt changes happened generally towards the end of each question, during most days the Brier scores were really high. Given that these problems were typically very long, they gained a higher weight under *Scores by Day* than under *Scores by Problem*. This explains why the *Scores by Day* are higher than the *Scores by Problem* under the columns *All Problems* and *Long*.

7.2. *In- and Out-of-Sample Sharpness and Calibration.* A calibration plot is a simple tool for assessing the sharpness and calibration of a model. The idea is to plot the probability forecasts against the observed empirical frequencies. Therefore any deviation from the diagonal line suggest poor calibration. A model is considered under-confident (or over-confidence) if the points form an S-shaped (or Ƨ-shaped) trend. In order to assess sharpness of the model, it is common practice to place a histogram of the given forecasts within the plot.

The top and bottom rows of Figure 3 present calibration plots for SDLM, STC-Log, STC-Bri, and BSTC-Log under in- and out-of-sample probability estimation, respectively. Each case is of interest in its own right: Good in-sample calibration is crucial for model interpretability. In particular, if the estimated crowd belief is well-calibrated, then the elements of the bias vector $\boldsymbol{b}$ can be used to study the amount of under- or over-confidence in the different expertise groups. Good out-of-sample calibration and sharpness, on other hand, are necessary properties in predicting future events with high accuracy. To guide our assessment, the dashed bands around the diagonal connect the point-wise, Bonferroni-corrected (Bonferroni (1936)) 95% lower and upper critical values under the null hypothesis of calibration. These have been computed by running the bootstrap technique described in Bröcker and Smith (2007) for 10,000 iterations. The in-sample results were obtained by running the models were for 10,200 iterations leading to a final posterior sample of 1,000 observations after thinning and using the first 200 iterations for burn-in. The out-of-sample results were computed based on the 10-fold cross-validation discussed in Section 7.1.

Overall, the *Sample-Then-Calibrate*-procedure is sharp and well-calibrated both in- and out-of-sample with only a few points barely falling outside the *point-wise* critical values. Since the

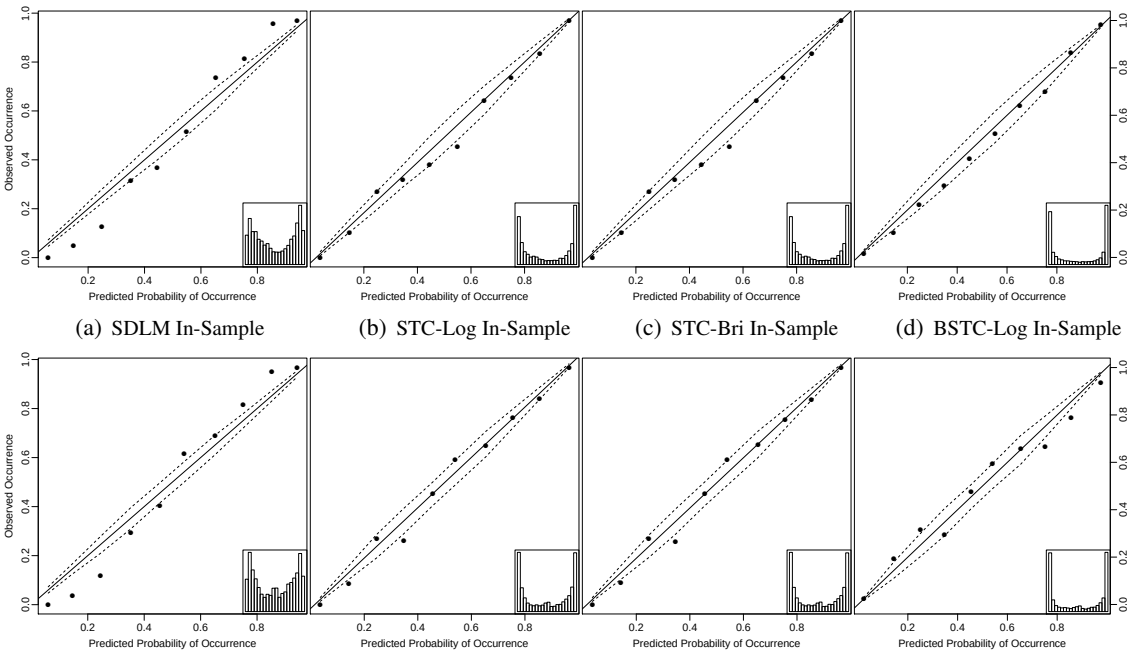

(a) SDLM In-Sample (b) STC-Log In-Sample (c) STC-Bri In-Sample (d) BSTC-Log In-Sample

(e) SDLM Out-of-Sample (f) STC-Log Out-of-Sample (g) STC-Bri Out-of-Sample (h) BSTC-Log Out-of-Sample

FIG 3. *The top and bottom rows show in- and out-of-sample calibration and sharpness, respectively. The models are Simple Dynamic Linear Model (SDLM), the Sample-Then-Calibrate approach that optimizes over the logarithmic score (STC-Log), the Sample-Then-Calibrate approach that optimizes over the Brier score (STC-Bri), and the fully-Bayesian version of the Sample-Then-Calibrate approach that optimizes over the logarithmic score (BSTC-Log).*

calibration does not change drastically from the top to the bottom row, the *Sample-Then-Calibrate*-procedure can be considered to present robustness against over-fitting. This is, however, not the case with BSTC-Log that is well-calibrated in-sample but presents over-confidence out-of-sample. Figures 3(a) and 3(e) serve as baselines by showing the reliability plots for the SDLM-model. Since this model does not perform any explicit calibration, it is not surprising to see most points outside the critical values. The pattern in the deviations suggests drastic under-confidence, and the inset histogram reveals drastic lack of sharpness.

7.3. *Group-Level Expertise Bias.* Recall from Section 2 that the experts were asked to self-assess their level of expertise (on a 1-to-5 scale with 1 = Not At All Expert to 5 = Extremely Expert) on any questions that they participated in. The self-reported expertise then divides the experts into 5 groups, with each group assigned a separate multiplicative bias term. This section uses the *Sample-Then-Calibrate*-procedure to explore the posterior distribution of these multiplicative bias terms. Figure 4 presents the posterior distributions of the bias terms with side-by-side box plots. Since the distributions fall completely below the *no-bias* reference-line at 1.0, all the groups are deemed under-confident.

The under-confidence, however, decreases as the level of expertise increases. For instance, the posterior probability that the most expert group is the least under-confident is approximately equal to 1.0, and the posterior probability of a strictly decreasing level of under-confidence is approximately 0.87. The latter probability is driven down by the inseparability of the two groups associated with the lowest levels of self-reported expertise. The fact that these groups are very similar suggests that the forecasters are poor at assessing how little they know about a subject that is strange to them. If these groups are combined into a single group, the posterior probability of a strictly decreasing level of under-confidence is approximately 1.0.

The decreasing trend in under-confidence can be reasoned by viewing the process of making a subjective probability as Bayesian updating: At first a completely ignorant expert aiming to minimize a reasonable loss function, such as the Brier score, has no reason to give anything but 0.5 as his probability forecast. However, as soon as the expert gains some knowledge about the event, he produces an updated forecast that is a compromise between his initial forecast and the new information acquired. The updated forecast is therefore conservative and too close to 0.5 as long as the expert remains only partially informed about the event. If most experts fall somewhere on this spectrum between ignorance and full information, their average forecast tends to fall strictly between 0.5 and the most-informed probability forecast (see Baron et al. (2013) for more details). Since expertise is to a large extent determined by subject-matter knowledge, the level of under-confidence can be expected to decrease as a function of the group's level of self-reported expertise.

Finding under-confidence in all the groups is a rather surprising result given that many previous studies have been conducted to show that experts are likely to be over-confident. For instance, Lichtenstein, Fischhoff and Phillips (1977); Morgan (1992); Bier (2004) summarize the results from numerous calibration studies, and conclude that experts are systematically over-condent about their probability assessments. Our result, however, is a statement about groups of experts and hence does not invalidate the possibility of the individual experts being overconfident. To make conclusions at the individual-level based on the group-level bias terms would be considered an *ecological inference fallacy* (see, e.g., Lubinski and Humphreys (1996)).

7.4. *Question Difficulty and Other Measures.* One advantage of our model arises from its ability to produce estimates of interpretable question-specific parameters γ_k, σ_k^2, and τ_k^2. These quantities can be combined in many interesting ways to answer questions about different groups of experts or the questions themselves. For instance, being able to assess the difficulty of a question could lead to more principled ways of aggregating performance measures across questions or to novel insight on the kind of questions that are found difficult by experts (see, e.g., a discussion on the *Hard-Easy Effect* in Wilson and Wilson (1994)). To illustrate, recall that higher values of σ_k^2 suggest greater disagreement among the participating experts. Since experts are more likely to disagree over a difficult question than an easy one, it is reasonable to assume that σ_k^2 has a positive relationship with question difficulty. An alternative measure is given by τ_k that quantifies the volatility of the underlying circumstances that ultimately decide the outcome of the event. Therefore a high value of τ_k can cause the outcome of the event appear unstable and difficult to predict.

As a final illustration of our model, consider the two questions used for illustrative purposes in

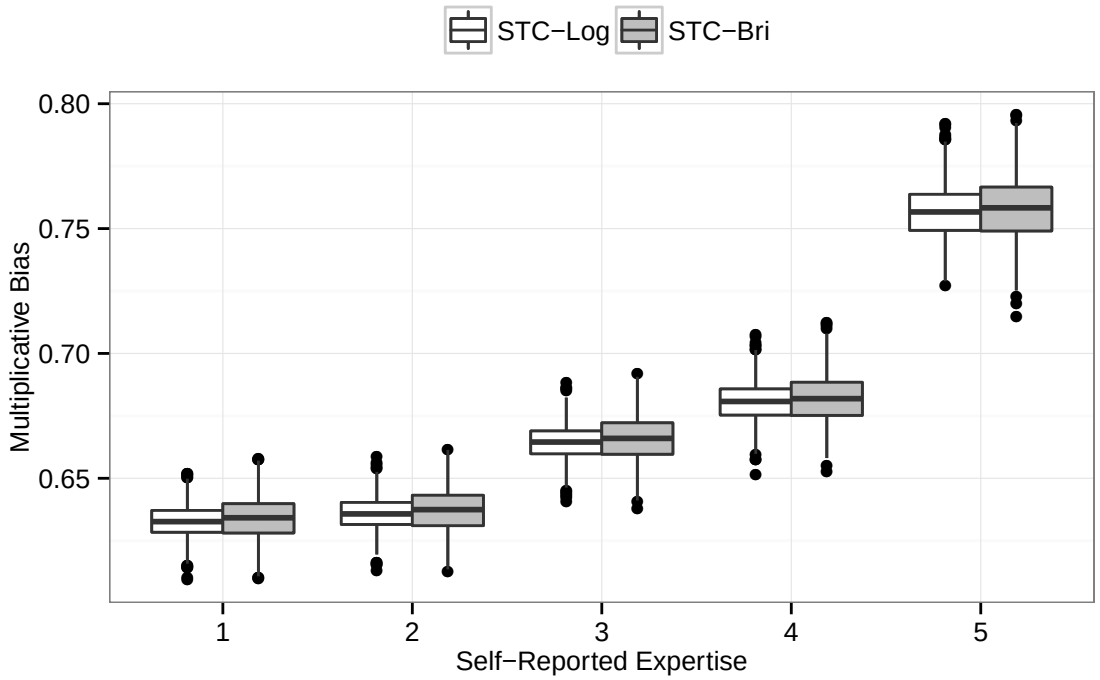

FIG 4. *Comparing the bias-levels across self-reported expertise under different approaches. Posterior distributions of* b_j *for* $j = 1, \ldots, 5$ *under the Sample-Then-Calibrate approach that optimizes over the logarithmic score and the Sample-Then-Calibrate approach that optimizes over the Brier score.*

Section 2. Figure 5 is a copy of Figure 1 with the addition of a solid line surrounded by a dashed band. The solid line represents the posterior mean of the calibrated crowd belief as estimated by STC-Log. The dashed lines connect the point-wise 95% posterior intervals across different time points. Since $\hat{\sigma}_k^2 = 2.43$ and $\hat{\sigma}_k^2 = 1.77$ for the questions depicted in Figures 5(a) and 5(b), respectively, the first question provokes more disagreement among the experts than the second one. Intuitively this makes sense because the target event in Figure 5(a) is determined by several conditions that may change radically from one day to the next while the target event in Figure 5(b) is determined by a relatively steady stock market index. Therefore it is not surprising to find that the first question has $\hat{\tau}_k^2 = 1.38$ while the second one has $\hat{\tau}_k^2 = 0.198$. We conclude that the first question can be considered inherently more difficult than the second one.

8. Discussion. This paper began with an introduction of a rather unorthodox but nonetheless realistic probability forecasting setting, in which forecasts are made very infrequently by a heterogeneous group of experts over a period of time. The resulting data is too sparse to be modeled

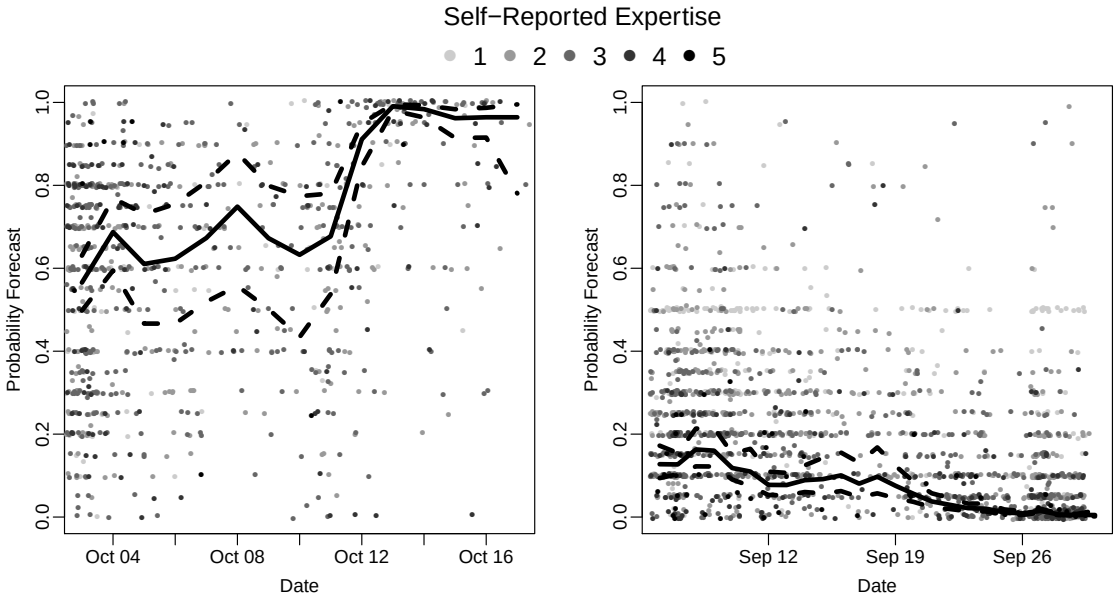

(a) *Will the expansion of the European bailout fund be ratified by all 17 Eurozone nations before 1 November 2011?*

(b) *Will the Nikkei 225 index finish trading at or above 9,500 on 30 September 2011?*

FIG 5. *Scatterplots of the probability forecasts given for two questions in our dataset. The shadings represents the self-reported expertise of the forecaster who provided the probability forecast. The solid line gives the posterior mean of the calibrated crowd belief as estimated by STC-Log. The surrounding dashed lines connect the point-wise 95% posterior intervals.*

efficiently with standard time-series methods. In response to this lack of appropriate methodology, our work introduces an interpretable time-series model that incorporates self-reported expertise and captures a sharp and well-calibrated crowd belief across time. The model is estimated in two-steps: The first step samples constrained versions of the model parameters via a Gibbs sampler that only makes use of standard distributions. The second step involves a one-dimensional optimization procedure that transforms the constrained parameter values into their unconstrained counterparts.

8.1. *Summary of Findings.* The model was applied to an unusually large dataset on probability forecasting done by human experts. The estimated crowd belief was found to be sharp and well-calibrated under both in- and out-of-sample probability estimation. This has direct implications on predictive power and model interpretability. Firstly, the model was shown to outperform other probability aggregators in terms of forecasting ability. Secondly, the crowd belief was used as the no-bias reference point to study the distributions of the bias terms for different expertise-groups. All the groups were found to be under-confident. The under-confidence, however, decreased as the level of self-reported expertise increased. This result is about groups of experts and hence does not conflict with the well-known result of the individuals being over-confident (see, e.g., Lichten-

stein, Fischhoff and Phillips (1977); Morgan (1992); Bier (2004)). Besides making predictions or studying group-level bias, the model can be used to generate estimates of many problem-specific quantities. These quantities have clear interpretations and can be combined in many interesting ways to answer a range of hypotheses about the experts and the questions.

8.2. *Future Directions and Limitations.* The model can be extended in different ways to meet a wide range of research objectives. For instance, the degree to which the group-level underconfidence decreases towards the resolution of the target event, could be studied by allowing the bias vector to depend on time. The model is also by no means limited to the study of group-level bias at different levels of self-reported expertise. The experts could equally well be partitioned based on other features, such as gender, education, or specialty, to produce a range of novel insight on the level of confidence among different groups of expert forecasters. Similarly, the model could be applied to questions grouped by types, such as economic, domestic, or international, to learn about expert forecasting under a wide variety of problem attributes.

Other future directions could aim to remove some of the obvious limitations of our model. For instance, recall that the random components are assumed to follow a normal distribution. This is a strong assumption that may not always be justified. Logit-probabilities, however, have been modeled with a normal distribution before (see, e.g., Erev, Wallsten and Budescu (1994)). Furthermore, the normal distribution is a rather standard assumption in psychological models (see, e.g., signal-detection theory in Tanner Jr and Swets (1954)). A second limitation resides in the assumption that both the observed and hidden processes are expected to grow linearly. This assumption could be relaxed, for instance, by adding higher order terms to the model. A more complex model, however, is likely to sacrifice interpretability. Given that our model is able to detect very intricate patterns in the crowd belief (see Figure 5), compromising interpretability for the sake of facilitating non-linear growth is hardly necessary.

APPENDIX A: TECHNICAL DETAILS OF THE SAMPLING STEP

The Gibbs sampler (Geman and Geman (1984)) iteratively samples all the unknown parameters from their full-conditional posterior distributions one block of parameters at a time. Since this is performed under the constraint $b_3 = 1$ to ensure model identifiability, the constrained parameter estimates should be denoted with a trailing (1) to maintain consistency with earlier notation. For instance, the constrained estimate of γ_k should be denoted by $\hat{\gamma}_k(1)$ while the unconstrained estimate is denoted by $\hat{\gamma}_k$. For the sake of clarity, however, the constraint suffix is omitted in this section. Nonetheless, it is important to keep in mind that all the estimates in this section are constrained.

Sample $X_{t,k}$

The hidden states are sampled via the *Forward-Filtering-Backward-Sampling* (FFBS) algorithm that first predicts the hidden states using a Kalman Filter and then performs a backward sampling procedure that treats these predicted states as additional observations (see, e.g., Carter and Kohn (1994); Migon et al. (2005) for details on FFBS). More specifically, the first part, namely the

Kalman Filter, is deterministic and consists of a predict and an update step. Given all the other parameters except the hidden states, the predict step for the kth question is

$$\begin{aligned} X_{t|t-1,k} &= \gamma_k X_{t-1|t-1,k} \\ P_{t|t-1,k} &= \gamma_k^2 P_{t-1|t-1,k} + \tau_k^2, \end{aligned}$$

where the initial values, $X_{0|0,k}$ and $P_{0|0,k}$, are equal to 0 and 1, respectively. The update step is

$$\begin{aligned} e_{t,k} &= Y_{i,t,k} - b_{i,k} X_{t|t-1,k} \\ S_{t,k} &= \sigma_k^2 + b_{i,k}^2 P_{t|t-1,k} \\ K_{t,k} &= P_{t|t-1,k} b_{i,k} S_{t,k}^{-1} \\ X_{t|t,k} &= X_{t|t-1,k} + K_{t,k} e_{t,k} \\ P_{t|t,k} &= (1 - K_{t,k} b_{i,k}) P_{t|t-1,k}, \end{aligned}$$

where $b_{i,k}$ is the corresponding bias term for the ith expert in the kth question. The update step is repeated sequentially for each observation $Y_{i,t,k}$ given at time t. For each such repetition of the update step, the previous posterior values, $X_{t|t,k}$ and $P_{t|t,k}$, should be considered as the new prior values, $X_{t|t-1,k}$ and $P_{t|t-1,k}$. After running the Kalman Filter up to the final time point at $t = T_k$, the final hidden state is sampled from $X_{T_k,k} \sim \mathcal{N}(X_{T_k|T_k,k}, P_{T_k|T_k,k})$. The remaining states are obtained via the backward sampling that is performed in reverse from

$$X_{t-1,k} \sim \mathcal{N}\left(V\left(\frac{\gamma_k X_{t,k}}{\tau_k^2} + \frac{X_{t|t,k}}{P_{t|t,k}}\right), V\right),$$

where

$$V = \left(\frac{\gamma_k^2}{\tau_k^2} + \frac{1}{P_{t|t,k}}\right)^{-1}$$

This can be viewed as backward updating that considers the Kalman Filter estimates as additional observations at each given time point. If the observation $\boldsymbol{Y}_{t,k}$ is completely missing at time t, the update step is skipped and the state estimates are sampled from

$$\mathcal{N}\left(\gamma_k X_{t-1|t-1,k}, \gamma_k^2 P_{t-1|t-1,k} + \tau_k^2\right)$$

Sample $\boldsymbol{b}$ and σ_k^2

First, vectorize all the response vectors $\boldsymbol{Y}_{t,k}$ into a single vector denoted $\boldsymbol{Y}_k = \left[\boldsymbol{Y}_{1,k}^T, \ldots, \boldsymbol{Y}_{T_k,k}^T\right]^T$. Since each $\boldsymbol{Y}_{t,k}$ is matched with $X_{t,k}$ via the time index t, we can form a $|\boldsymbol{Y}_k| \times J$ design-matrix by letting $\boldsymbol{X}_k = \left[(\boldsymbol{M}_k X_{1,k})^T, \ldots, (\boldsymbol{M}_k X_{T_k,k})^T\right]^T$. Given that the goal is to borrow strength across questions by assuming a common bias vector $\boldsymbol{b}$, the parameter values must be

estimated in parallel for each question such that the matrices $\boldsymbol{X}_k$ can be further concatenated into $\boldsymbol{X} = [\boldsymbol{X}_1^T, \ldots, \boldsymbol{X}_K^T]^T$ during every iteration. Similarly, $\boldsymbol{Y}_k$ must be further vectorized into a vector $\boldsymbol{Y} = [\boldsymbol{Y}_1^T, \ldots, \boldsymbol{Y}_K^T]^T$. The question-specific variance terms are taken into account by letting $\boldsymbol{\Sigma} = \text{diag}(\sigma_1^2 \mathbf{1}_{1\times T_1}, \ldots, \sigma_K^2 \mathbf{1}_{1\times T_K})$. After adopting the non-informative prior $p(\boldsymbol{b}, \sigma_k^2 | \boldsymbol{X}_k) \propto \sigma_k^{-2}$ for each $k = 1, \ldots, K$, the bias vector are sampled from

$$\boldsymbol{b}|\ldots \;\sim\; \mathcal{N}_J\left((\boldsymbol{X}^T\boldsymbol{\Sigma}^{-1}\boldsymbol{X})^{-1}\boldsymbol{X}^T\boldsymbol{\Sigma}^{-1}\boldsymbol{Y}, (\boldsymbol{X}^T\boldsymbol{\Sigma}^{-1}\boldsymbol{X})^{-1}\right) \tag{6}$$

Since the covariance matrix in Equation (6) is diagonal, the constraint is enforced at this point by letting $b_3 = 1$. The variance parameter is then sampled from

$$\sigma_k^2|\ldots \;\sim\; \text{Inv-}\chi^2\left(|\boldsymbol{Y}_k| - J, \frac{1}{|\boldsymbol{Y}_k| - J}(\boldsymbol{Y}_k - \boldsymbol{X}_k\boldsymbol{b})^T(\boldsymbol{Y}_k - \boldsymbol{X}_k\boldsymbol{b})\right),$$

where the distribution is a scaled inverse-χ^2 (see, e.g., Gelman et al. (2003)). Since the experts are not required to give a new prediction at every time unit, the design matrices must be trimmed accordingly such that their dimensions match up with the dimensions of the observed matrices.

Sample γ_k and τ_k^2

Estimating the parameters related to the hidden process are estimated via a regression setup. More specifically, after adopting the non-informative prior $p(\gamma_k, \tau_k^2 | \boldsymbol{X}_k) \propto \tau_k^{-2}$, the parameter values are sampled from

$$\begin{aligned}
\gamma_k|\ldots \;&\sim\; \mathcal{N}\left(\frac{\sum_{t=2}^{T_k} X_{t,k}X_{t-1,k}}{\sum_{t=1}^{T_k-1} X_{t,k}^2}, \frac{\tau_k^2}{\sum_{t=1}^{T_k-1} X_{t,k}^2}\right) \\
\tau_k^2|\ldots \;&\sim\; \text{Inv-}\chi^2\left(T_k - 1, \frac{1}{T_k - 1}\sum_{t=2}^{T_k}(X_{t,k} - \gamma_k X_{t-1,k})^2\right),
\end{aligned}$$

where the final distribution is a scaled inverse-χ^2 (see, e.g., Gelman et al. (2003)).

REFERENCES

ALLARD, D., COMUNIAN, A. and RENARD, P. (2012). Probability Aggregation Methods in Geoscience. *Mathematical Geosciences* **44** 545-581.

ARIELY, D., AU, W. T., BENDER, R. H., BUDESCU, D. V., DIETZ, C. B., GU, H., WALLSTEN, T. S. and ZAUBERMAN, G. (2000). The effects of averaging subjective probability estimates between and within judges. *Journal of Experimental Psychology: Applied* **6** 130-147.

BAARS, J. A. and MASS, C. F. (2005). Performance of National Weather Service forecasts compared to operational, consensus, and weighted model output statistics. *Weather and forecasting* **20** 1034–1047.

BARON, J., UNGAR, L. H., MELLERS, B. A. and E., T. P. (2013). Two reasons to make aggregated probability forecasts more extreme. *submitted.*

BIER, V. (2004). Implications of the research on expert overconfidence and dependence. *Reliability Engineering & System Safety* **85** 321–329.

BONFERRONI, C. E. (1936). Teoria statistica delle classi e calcolo delle probabilitá. *Pubblicazioni del R Istituto Superiore di Scienze Economiche e Commerciali di Firenze* **8** 3-62.

BRIER, G. W. (1950). Verification of Forecasts Expressed in Terms of Probability. *Monthly Weather Review* **78** 1-3.

BRÖCKER, J. and SMITH, L. A. (2007). Increasing the reliability of reliability diagrams. *Weather and Forecasting* **22** 651–661.

BUJA, A., STUETZLE, W. and SHEN, Y. (2005). Loss functions for binary class probability estimation and classification: Structure and applications. *Working draft, November*.

CARTER, C. K. and KOHN, R. (1994). On Gibbs sampling for state space models. *Biometrika* **81** 541–553.

CHEN, Y. (2009). Learning Classifiers from Imbalanced, Only Positive and Unlabeled Data Sets. *Department of Computer Science Iowa State University*.

CLEMEN, R. T. and WINKLER, R. L. (2007). Aggregating probability distributions. *Advances in Decision Analysis* 154–176.

COOKE, R. M. (1991). Experts in uncertainty: opinion and subjective probability in science.

EREV, I., WALLSTEN, T. S. and BUDESCU, D. V. (1994). Simultaneous Over- and Underconfidence: The Role of Error in Judgment Processes. *Psychological Review* **66** 519-527.

GELMAN, A., CARLIN, J. B., STERN, H. S. and RUBIN, D. B. (2003). *Bayesian data analysis*. CRC press.

GELMAN, A., JAKULIN, A., PITTAU, M. G. and SU, Y.-S. (2008). A weakly informative default prior distribution for logistic and other regression models. *The Annals of Applied Statistics* 1360–1383.

GEMAN, S. and GEMAN, D. (1984). Stochastic relaxation, Gibbs distributions, and the Bayesian restoration of images. *Pattern Analysis and Machine Intelligence, IEEE Transactions on* **6** 721–741.

GENEST, C. and ZIDEK, J. V. (1986). Combining Probability Distributions: A Critique and an Annotated Bibliography. *Statistical Science* **1** 114-148.

GENT, I. P. and WALSH, T. (1996). Phase transitions and annealed theories: Number partitioning as a case study'. In *ECAI* 170–174. Citeseer.

GNEITING, T., STANBERRY, L. I., GRIMIT, E. P., HELD, L. and JOHNSON, N. A. (2008). Rejoinder on: Assessing probabilistic forecasts of multivariate quantities, with an application to ensemble predictions of surface winds. *Test* **17** 256–264.

GOOD, I. J. (1952). Rational decisions. *Journal of the Royal Statistical Society. Series B (Methodological)* 107–114.

HASTINGS, C., MOSTELLER, F., TUKEY, J. W. and WINSOR, C. P. (1947). Low moments for small samples: a comparative study of order statistics. *The Annals of Mathematical Statistics* **18** 413–426.

HAYES, B. (2002). The easiest hard problem. *American Scientist* **90** 113–117.

KARMARKAR, N. and KARP, R. M. (1982). *The differencing method of set partitioning*. Computer Science Division (EECS), University of California Berkeley.

KELLERER, H., PFERSCHY, U. and PISINGER, D. (2004). *Knapsack problems*. Springer.

LICHTENSTEIN, S., FISCHHOFF, B. and PHILLIPS, L. D. (1977). *Calibration of probabilities: The state of the art*. Springer.

LUBINSKI, D. and HUMPHREYS, L. G. (1996). Seeing the forest from the trees: When predicting the behavior or status of groups, correlate means. *Psychology, Public Policy, and Law* **2** 363.

METROPOLIS, N., ROSENBLUTH, A. W., ROSENBLUTH, M. N., TELLER, A. H. and TELLER, E. (1953). Equation of state calculations by fast computing machines. *The journal of chemical physics* **21** 1087.

MIGON, H. S., GAMERMAN, D., LOPES, H. F. and FERREIRA, M. A. (2005). Dynamic models. *Handbook of Statistics* **25** 553–588.

MILLS, T. C. (1991). *Time series techniques for economists*. Cambridge University Press.

MORGAN, M. G. (1992). *Uncertainty: a guide to dealing with uncertainty in quantitative risk and policy analysis*. Cambridge University Press.

NEAL, R. M. (2003). Slice sampling. *Annals of statistics* 705–741.

NICULESCU-MIZIL, A. and CARUANA, R. (2005). Obtaining Calibrated Probabilities from Boosting. In *UAI* 413.

PEPE, M. S. (2003). The statistical evaluation of medical tests for classification and prediction.

PLATT, J. et al. (1999). Probabilistic outputs for support vector machines and comparisons to regularized likelihood methods. *Advances in large margin classifiers* **10** 61–74.

PRIMO, C., FERRO, C. A., JOLLIFFE, I. T. and STEPHENSON, D. B. (2009). Calibration of probabilistic forecasts of binary events. *Monthly Weather Review* **137** 1142–1149.

RAFTERY, A. E., GNEITING, T., BALABDAOUI, F. and POLAKOWSKI, M. (2005). Using Bayesian model averaging to calibrate forecast ensembles. *Monthly Weather Review* **133** 1155–1174.

RANJAN, R. and GNEITING, T. (2010). Combining Probability Forecasts. *Journal of the Royal Statistical Society: Series B (Statistical Methodology)* **72** 71-91.

SANDERS, F. (1963). On subjective probability forecasting. *Journal of Applied Meteorology* **2** 191–201.

SATOPÄÄ, V. A., BARON, J., FOSTER, D. P., MELLERS, B. A., TETLOCK, P. E. and UNGAR, L. H. (2013). Combining Multiple Probability Predictions Using a Simple Logit Model. *submitted*.

SHLYAKHTER, A. I., KAMMEN, D. M., BROIDO, C. L. and WILSON, R. (1994). Quantifying the credibility of energy projections from trends in past data: The US energy sector. *Energy Policy* **22** 119–130.

TANNER JR, W. P. and SWETS, J. A. (1954). A decision-making theory of visual detection. *Psychological review* **61** 401.

TETLOCK, P. E. (2005). *Expert political judgment: How good is it? How can we know?* Princeton University Press.

UNGAR, L., MELLERS, B., SATOPÄÄ, V., TETLOCK, P. and BARON, J. (2012). The Good Judgment Project: A Large Scale Test of Different Methods of Combining Expert Predictions. In *2012 AAAI Fall Symposium Series*.

VISLOCKY, R. L. and FRITSCH, J. M. (1995). Improved model output statistics forecasts through model consensus. *Bulletin of the American Meteorological Society* **76** 1157–1164.

WALLACE, B. C. and DAHABREH, I. J. (2012). Class probability estimates are unreliable for imbalanced data (and how to fix them). In *Data Mining (ICDM), 2012 IEEE 12th International Conference on* 695–704. IEEE.

WALLSTEN, T. S., BUDESCU, D. V. and EREV, I. (1997). Evaluating and combining subjective probability estimates. *Journal of Behavioral Decision Making* **10** 243–268.

WILSON, A. G. and WILSON, A. G. (1994). Cognitive Factors Affecting Subjective Probability Assessment.

WILSON, P. W., DAGOSTINO, R. B., LEVY, D., BELANGER, A. M., SILBERSHATZ, H. and KANNEL, W. B. (1998). Prediction of coronary heart disease using risk factor categories. *Circulation* **97** 1837–1847.

WINKLER, R. L. and MURPHY, A. H. (1968). Good Probability Assessors1.

WRIGHT, G., ROWE, G., BOLGER, F. and GAMMACK, J. (1994). Coherence, calibration, and expertise in judgmental probability forecasting. *Organizational Behavior and Human Decision Processes* **57** 1–25.

PHILADELPHIA, PA 19104- 6340, USA
E-MAIL: satopaa@wharton.upenn.edu